HADRONIC PHYSICS
AT DAΦNE WITH THE KLOE DETECTOR

A. Antonelli
INFN, LNF
Frascati, Italy 00044

and

KLOE Collaboration *

ABSTRACT

Scalar mesons are poorly described by current models, in particular the narrow scalar mesons below 1 GeV, and more information is needed. At the Frascati National Laboratories a new ϕ-factory, DAΦNE, and a general purpose detector, KLOE, are under construction. The high luminosity provided by the machine (10^{33} cm^{-2} s^{-1}) will give a unique opportunity to study the $f_0(975)$ and $a_0(980)$ in the ϕ radiative decays. A complete MC study (including derivations of energy and angular distributions of the signals and backgrounds) has shown that even branching ratios as low as 10^{-6} can be measured. Clear cut indication will come from these measurements. Furthermore DAΦNE will give an excellent opportunity to study $\gamma\gamma$ reactions at low energy with high statistics, offering a clean test of chiral theories.

1. The DAΦNE Project

The DAΦNE [1] project (Double Annular ϕ-factory for Nice Experiments) has been approved in June 90 by the Italian Institute for Nuclear Physics (INFN). It is totally funded, the commissioning is planned for the end of 96 and it will be installed in the present ADONE building at the Frascati National Laboratories.

DAΦNE is an e^+e^- collider optimized to work at the ϕ mass with a goal luminosity L= 10^{33} cm^{-2}s^{-1}. The strategy to reach the target luminosity is to obtain the same

*A. Aloisio, A. Andryakov, A. Antonelli, M. Antonelli, F. Anulli, C. Avanzini, D. Babusci, C. Bacci, R. Baldini-Ferroli, G. Barbiellini, M. Barone, K. Barth, V. Baturin, H. Beker, G. Bencivenni, S. Bertolucci, C. Bini, C. Bloise, V. Bocci, V. Bolognesi, F. Bossi, L. Bucci, A. Calcaterra, R. Caloi, P. Campana, G. Capon, M. Carboni, G. Cataldi, S. Cavaliere, L. Cerrito, M. Cerù, F. Cervelli, F. Cevenini, G. Chiefari, M. Cordelli, P. Creti, F. Donno, R. De Sangro, P. De Simone, G. De Zorzi, A. Denig, G. Di Cosimo, A. Di Domenico, E. Drago, V. Elia, O. Erriquez, A. Farilla, G. Felici, A. Ferrari, M. L. Ferrer, G. Finocchiaro, D. Fiore, P. Franzini, A. Gaddi, C. Gatto, P. Gauzzi, E. Gero, S. Giovanella, E. Gorini, F. Grancagnolo, W. Grandegger, U. v. Hagel, R. Haydar, M. Imhof, M. Incagli, C. Joram, L. Keeble, W. Kim, W. Kluge, F. Lacava, G. Lanfranchi, P. Laurelli, J. Lee-Franzini, A. Martini, A. Martinis, M. M. Massai, R. Messi, L. Merola, A. Michetti, S. Miscetti, S. Moccia, F. Murtas, M. Napolitano, E. Pace, G. F. Palamà, M. Panareo, L. Paoluzi, A. Parri, E. Pasqualucci, M. Passaseo, A. Passeri, V. Patera, F. Pelucchi, E. Petrolo, M. C. Petrucci, M. Piccolo, M. Pollack, L. Pontecorvo, M. Primavera, F. Ruggieri, P. Santantonio, R. D. Schamberger, F. Scuri, A. Smilzo, S. Spagnolo, E. Spiriti, C. Stanescu, L. Tortora, P. M. Tuts, E. Valente, P. Valente, G. Venanzoni, S. Veneziano, X. L. Wang, S. Weseler, R. Wieser, S. Wölfle, A. Zallo.

single bunch luminosity achieved at VEPP-2M and to increase the number of bunches (up to 120). To suppress multibunch instabilities the electrons and the positrons will circulate in two separate storage rings and they will collide at two interaction points with a horizontal half angle of 10 mrad. In the interaction regions, equipped with two triplets of low-β quadrupoles, two experiments will be installed: KLOE, mainly for CP violation studies, and FINUDA, mainly for hypernuclei and low energy KN interactions studies. Some machine parameters are reported in Table 1.

Table 1: DAΦNE machine parameters.

Total CM energy (GeV)	1.0	Luminosity (10^{32} cm^{-2} s^{-1})	1.00 - 10
Bunches per ring per beam	30 - 120	Particles/bunch	8.9×10^{10}
Luminosity lifetime (hr's)	2 - 3	Single ring circumference	97.69 m
Time between collisions (ns)	10.9 - 2.7	Crossing half-angle (mrad)	10 - 15
β-function at IP: H	4.5 m	β-function at IP: V	4.5 cm
Beam r.m.s. size at IP: H	2.1 mm	Beam r.m.s. size at IP: V	21 μm
Energy loss/turn (KeV)	9.3	Rel. nat. r.m.s. energy spread	4×10^{-4}
r.m.s. bunch length (cm)	3.0	Nat. emittance (mm $\times$ mrad)	1.0

2. The KLOE Detector

The KLOE [2 3] detector has been designed primarily with the goal of detecting CP violation in K^0 decays. It is composed by a superconductive solenoid that will provide a magnetic field of 6 KG, a central drift chamber and an electromagnetic calorimeter installed inside the coil.

2.1. The Tracking Chamber.

The main tasks of the tracking system are:

• Large radius and homogeneous volume to collect as many K_L decays as possible, taking into account that the K_L mean decay lenght is 3.5 m.

• Optimized resolution for low momentum tracks by using light gas and light walls to minimize multiple scattering, regeneration and γ's conversion.

We have chosen a 2 m radius and 3.5 m long drift chamber with cell configuration almost square, $3\times$ 3 cm^2 effective area. To fill uniformly the sensitive volumes only stereo wires will be used with a stereo angle that varies with radius from 50 mrad to 120 mrad going outward. The gas mixture will be helium with the usual addition of hydrocarbons for a total radiation length of $\sim$500 m, including the wires.

The performances obtained with a small prototype are: $\sigma_{r,\phi} < 200$ μm, and a cell efficiency > 99 %, corresponding to a momentum resolution $\sigma_{P_t}/\mathrm{P}_t\sim 0.3$ %.

A large prototype has been built and will be tested in November.

2.2. The Electromagnetic Calorimeter.

To discriminate between $K_L \to \pi^0\pi^0 / K_L \to \pi^0\pi^0\pi^0$ the calorimeter should have first of all full efficiency for γ's in the energy range 20–280 MeV. Of course hermeticity and a good energy resolution are also demanded. The calorimeter should also provide a fast trigger and should have a reasonable cost. Good time performance is also very useful to reconstruct the K_L neutral vertex with high resolution.

We have chosen to use a lead-scintillator sampling calorimeter consisting of 0.5 mm lead layer in which 1 mm diameter scintillating fibers are embedded. The calorimeter is composed of a central part (barrel), with an inner radius of 2 m, a thickness of 23 cm ($\sim 15 X_0$) and a length of 4.3 m, and two end-caps that close hermetically the calorimeter. The total acceptance is 98 % of the full solid angle. The read-out is organized in five layers of twelve 4.5×4.5 cm cells coupled with two photomultipliers by light guides. The spatial resolution in reconstructing the shower apex is $\sigma_x \sim \sigma_y \sim 1.2$ cm and $\sigma_z \sim 2.5$ cm obtained by time difference.

A four meter long module has been built and tested with electrons, photons, muon and pion beams. The achieved performances are:

- $\sigma(E)/E \sim 4.4\%/\sqrt{E\ (GeV)}$
- $\sigma_T \sim 34$ ps$/\sqrt{E\ (GeV)}$.
- Very good linearity in the energy range of interest.
- No deterioration in the resolutions and in the response in function of the incidence angle.
- Some capability for distinguishing between pions and muons.

In conclusion, the tests indicate that our design more than meets the specifications.

3. Scalar Mesons $f_0(975)$ and $a_0(980)$ puzzle

3.1. Introduction

Although the scalar mesons $f_0(975)$ and $a_0(980)$ are well established their physical nature is still unclear. The first evidence for the f_0 was in the reaction p$\pi \to \pi\pi$n: a narrow dip coupled with a sharp onset of inelasticity in the I=J=0 $\pi\pi$ elastic cross section indicated the presence of a dynamical structure strongly coupled to $K\overline{K}$. Moreover it has been seen in the J/ψ radiative decays by the DM2 and MARK III collaborations, the $\gamma\gamma$ width has been measured, it appears in the $\pi\pi$ invariant mass in the inclusive Z^0 decays and in the D_s decay. For the a_0 the first evidence was found in the $\eta\pi$ system in Kp$\to\Sigma\pi\eta$. Now there are very accurate data from Crystal Barrel and GAMS and the $\gamma\gamma$ width has also been measured. In conclusion we are in presence of two scalar mesons very close in mass, with a small width and a small $\gamma\gamma$ coupling. So which is the nature of such states? The standard $q\bar{q}$, $\rho-\omega$ like mesons, interpretation is not favoured. The total widths are too small, we expect $\sim$500 MeV with respect to the observed 30 MeV. The $K\overline{K}$ coupling is too large for an OZI forbidden decay and the $\gamma\gamma$ partial width found is a factor 10–20 smaller than the $q\bar{q}$

predictions. A lot of possible interpretations are then coming out:

- $K\overline{K}$ molecule [4] that could explain width, $s\bar{s}$ coupling, $\gamma\gamma$ partial width
- $qq\overline{q}\overline{q}$ bag state [5]
- glueball in the f_0 case [6]
- A peculiar model by Gribov [7]
- Quarkonium states, where the f_0 is an $s\bar{s}$ state and the a_0 an $u\overline{d}$ one.

Pennington's [8] calculations, based on the number of nearby poles of the associated scattering amplitude in the complex energy plane, using all the existing data disfavour the $K\overline{K}$ molecule interpretation.

So it is clear that there is an urgent need to clarify the theoretical situation.

Table 2: $\phi \to \gamma a_0$, f_0 theoretical predictions.

Model	BR($\phi \to \gamma a_0$)/BR($\phi \to \gamma f_0$)	absolute BR
$K\overline{K}$molecule	1	$\sim 4\times 10^{-5}$
$qq\overline{q}\overline{q}$	1 – 9	$<10^{-6}$
$f_0 = s\bar{s}$	~ 0	$\sim 10^{-5}$
f_0 glueball,a_0 $q\bar{q}$	–	$<10^{-6}$

The ϕ–factory appears a very suitable place to solve the puzzle. In fact the absolute rates for $\phi \to \gamma f_0$, $\phi \to \gamma a_0$ and the ratio of this two rates differ significantly for the different interpretations. For a $K\overline{K}$ molecule model the ratio should be ~ 1 and the $\phi \to \gamma f_0$ branching ratio should be $\sim 4\times 10^{-5}$, on the contrary for a glueball the branching ratio should be small due to the double OZI suppression, for $qq\overline{q}\overline{q}$ state the ratio depend on the internal arrangement of the quarks inside the bag. [9] The predictions for the different models are reported in Table 2.

In conclusion the theoretical expectations for the rates range from 10^{-4}–10^{-6}. At present only an experimental upper limit of 10^{-3} is avalaible.

4. $\phi \to \gamma$ f_0 at DAΦNE with KLOE

To study the $\phi \to \gamma$ f_0 decay a complete simulation of the KLOE detector including realistic resolutions has been done [10]. The signal has been generated for different branching ratios and we have taken into account all possible sources of backgrounds.

4.1. $f_0 \to \pi^0\pi^0$

The signature of such decay is five photons detected in the calorimeter, one of them is a low energy photon ($\sim$50 MeV).

The background to this process come essentially from:

- $\phi \to \gamma$ $\pi^0\pi^0$ non resonant production with an experimental upper limit rate of 10^{-3} and a theoretical prediction of 10^{-5}.

• $\phi \rightarrow \rho^o\ \pi^0 (\rho^o \rightarrow \pi^0\gamma,\ \eta\gamma)$ with rates 3×10^{-5} and 6×10^{-6} respectively .

The backgrounds from processes $\phi \rightarrow \eta\gamma$ ($\eta \rightarrow \pi^0\pi^0\pi^0$) and $\phi \rightarrow K_S,\ K_L(K_S \rightarrow \pi^0\pi^0\pi^0$, $K_L \rightarrow \pi^0\pi^0)$ where two or five photons are not detected can be neglected due to the high hermeticity of the calorimeter.

The signal events can be easily selected by means of a kinematic fit imposing total energy and momentum conservation, requiring that four of the five photons are paired into two π^0's and requiring that the energy of the leftover photon is to be less than 100 MeV. The efficiencies on the signal and on the backgrounds respectively are: ϵ_{f_0} $\sim$65% ,$\epsilon_{\pi^0\pi^0\gamma}$ $\sim$0.13% and $\epsilon_{\rho^o\pi^0}$ $\sim 8\times\ 10^{-4}$.

The photon energy spectraum after the cuts has been fitted to polynomial for the background and to a Breit-Wigner for the signal, the background subtraction has been taken into account in the fractional error extimation on the BR measurement. So in one year running with a luminosity L= 5×10^{32} cm^{-2} s^{-1} and assuming a BR($\phi \rightarrow \gamma$ f$_0$) = 10^{-4} we will collect 350000 $\gamma\pi^0\pi^0$events corresponding to a fractional error Δ(BR)/BR $\sim$0.4 %. For smaller rates, BR = 10^{-6}, our error is $\sim$5 %. In conclusion we have a good sensitivity to the signal over the whole range of BR's examined.

4.2. $f_0 \rightarrow \pi^+\pi^-$

The signature for this process is a pair of nearly collinear charged pion and one low energy photon. In the $\pi^+\pi^-$channel additional backgrounds are present. The main contributions are coming from:

• $\pi^+\pi^-\gamma$ where the photon is irradiated by the electron (positron), Initial State Radiation (ISR), with a BR $\sim10^{-3}$.

• $\mu\mu\gamma$, where the muons are mistaken for a pion, with a BR $\sim10^{-3}$

• $\pi^+\pi^-\gamma$ where the photon is irradiated from the pions, Final State Radiation (FSR), with a BR $\sim10^{-4}$.

In this last case the pion pair is produced in a state with C=+1 and its amplitude (A$_1$) interferes with the signal one (A$_{f_0}$) alterating the f$_0$ signal both in shape as in magnitude.

The $\phi \rightarrow \pi^+\pi^-\pi^0$, $\rho\pi$ background can be rejected, despite their large BR's, using the KLOE's hermeticity.

To select the signal events additional cuts on the angle between the photon and the electron to reject ISR and the photon and the pion for FSR have been applied. The $\mu\mu\gamma$ background can be reduced by cutting on the difference between the measured photon energy and the one calculated from the charged tracks momemta assuming the pion mass.

As we have already mentioned the interference between the signal and the FSR amplitudes plays a fundamental role in the branching ratio measurement. Depending on the BR values and on the unknown sign of the interference the f$_0$ signal can become very small and some calculations [10] have shown that we will loose sensitivity for BR $< 5\times10^{-7}$. For small $\phi \rightarrow \gamma$ f$_0$ rate the interference amplitude dominates over the f$_0$ one and the reverse is true for large BR. For BR $\sim 1.75\times\ 10^{-4}$ the integrated contribution to the $\gamma\pi^+\pi^-$cross section vanishes, anyway the presence of the signal can be recognized by looking at the shape of the photon spectrum.

As an example in Fig.1 a,b,c,d the cross section for the signal, the interference term and signal plus the interference for the constructive and destructive case respectively is reported assuming a BR $=2.5\times10^{-4}$.

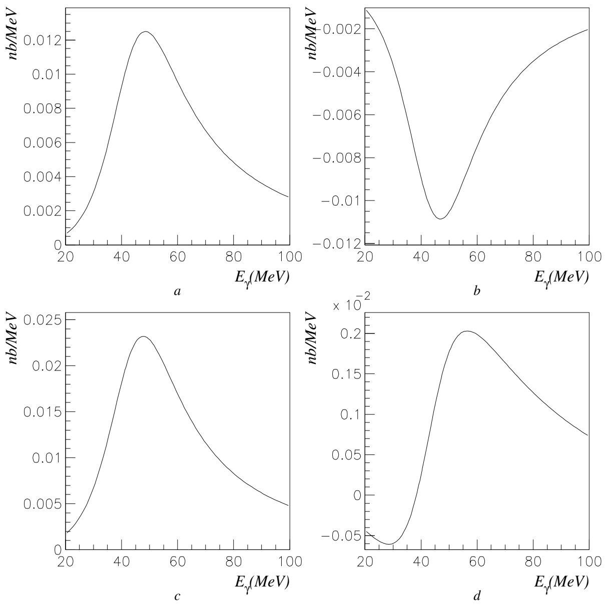

Figure 1: (a)γ spectrum for $|A_{f0}|^2$, (b) 2Re(A$_1$,A$_{f0}$), (c)$|A_{f0}|^2$−2Re(A$_1$,A$_{f0}$), (d) $|A_{f0}|^2$+2Re(A$_1$,A$_{f0}$)

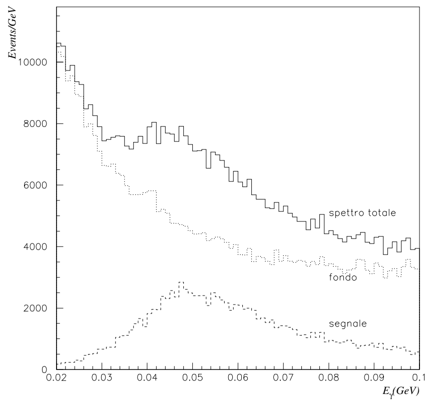

Figure 2: total γ spectrum (solid line), background spectrum (dotted line), signal spectrum (dashed line)

In Fig. 2 the photon spectrum that we will obtain in one year of running with a luminosity L= 5×10^{32} cm^{-2} s^{-1} assuming a BR $=\times10^{-4}$ and constructive interference is shown . The f_0 signal is clearly visible.

In conclusion this study has shown that also for the $\pi^+\pi^-$channel the $\phi \rightarrow\gamma$ f_0 rate down to 10^{-6} can be measured at DAΦNE with the KLOE detector. In one year running, the obtained accuracy being: 17 % for BR $\sim 10^{-6}$ and 0.5 % for BR $\sim 10^{-4}$.

5. $\gamma\gamma$ Physics At DAΦNE by $e^+e^-\rightarrow e^+e^-$ X

5.1. Introduction.

DAΦNE will offer an excellent possibility to study $\gamma\gamma$ interactions at low energy with high statistic [11]. Among the various topics we will discuss the possibilities of precise measurement of the $\gamma\gamma$ cross section and the studies of the e–π azimuthal correlations. This will allow to test chiral perturbation theories and techniques.

The existing measurements on $\gamma\gamma$ interactions at low energy are affected by large statistical and systematic uncertainties mainly due to the low available luminosity and to the relatively large background contribution. Moreover the data from different experiments do not agree very well and the comparison with theoretical calculations is difficult. In Fig. 3 the situation for $\gamma\gamma \rightarrow\pi^+\pi^-$,$\pi^0\pi^0$ together with the theoretical predictions is reported. For the $\pi^+\pi^-$mode MARK II [13] data agrees quite well with chiral prediction but for the DM1 [14], DM2 [15], PLUTO [16] data the agreement is very poor.

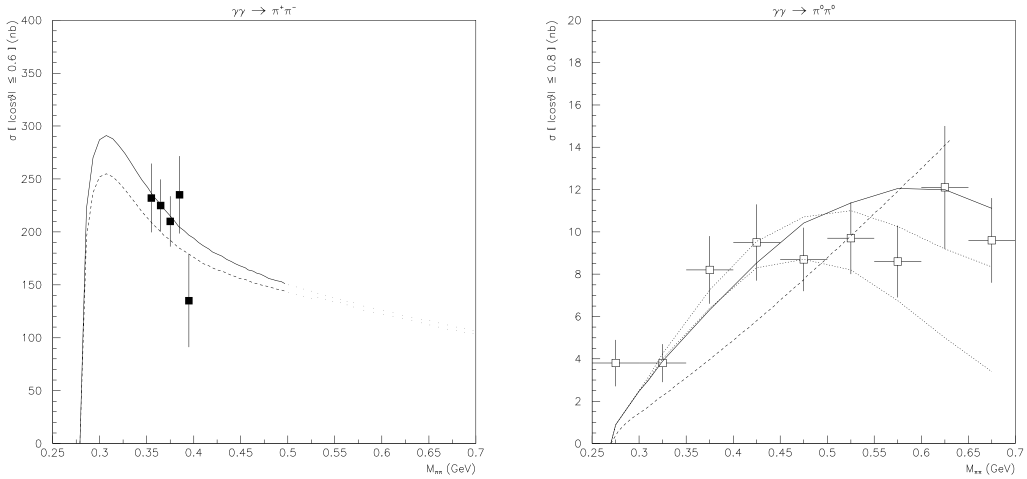

(a) (b)

Figure 3: (a):$\gamma\gamma \rightarrow \pi^+\pi^-$ (Born dashed line) (χPT solid line), (b):$\gamma\gamma \rightarrow \pi^0\pi^0$, χPT one loop (dashed line), χPT two loop (solid line) , Pennington predictions (dotted line)

For the $\pi^0\pi^0$mode we have only data from Crystal Ball [17] and in this case chiral calculations at tree level do not fit very well the data, better agreement is found including a two loop correction [18] and in the case of Pennington's [19] calculation based on unitarity.

Part of the previous problems are absent at DAΦNE due to:

• High $\gamma\gamma$ luminosity at low $\gamma\gamma$ mass. It can be seen from Fig. 4 that we will be competitive with LEP up to 600 MeV.

• Good tagging efficiency due to the relativly large outgoing electron angle, $\theta_e \sim m_e/E \sim 1$ mrad to be compared with 10^{-2} mrad of PEP and PETRA. This will allow to work in an almost background free enviroment, with the consequent reduction of systematic errors, and to study the azimuthal e–π correlations that so far could not be performed at existing colliders.

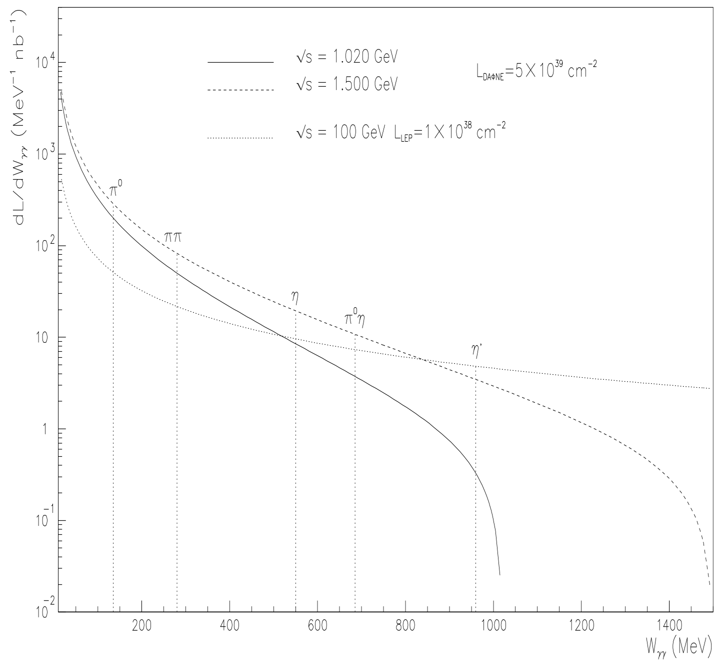

Figure 4: Photon-photon luminosity at DAΦNE as function of $\gamma\gamma$ mass

The available mass range at DAΦNE for the study of these processes is from threshold up to ~600 MeV and in one year running for a luminosity L $\sim 5\times10^{32}$ cm^{-2} s^{-1} 10^4 $\pi^0\pi^0$and 10^6 $\pi^+\pi^-$will be produced, a data sample two orders of magnitude larger than the Crystal Ball one.

5.2. $\gamma\gamma \to \pi\pi$ by KLOE.

One problem of measuring $\gamma\gamma \to \pi\pi$ at DAΦNE is the presence of a large background from $\phi \to K_S K_L (K_S \to \pi\pi)$ where the K_L escapes the detector. The cross section for such process is $\sigma \sim 100$ nb to be compared with 0.01 nb for $\gamma\gamma$ reaction. So even if some kinematic cut can help in reducing the backgruond the tagging of the electron (positron) is needed.

The proposed tagging system is composed by a small angle detector, SAT, installed downstream the Split Field Magnet and a wide angle detector, WAT, composed by KLOE itself with an additional small detector in front of the first low–β quadrupole. The angular acceptance is up to 10 mrad for the SAT and from 100 mrad on for the WAT. The single and double tagging efficiencies for the SAT are 40 % and 15 % respectively. In the SAT detector also electrons from radiative Bhabha reactions are present so that accidental coincidences can decrease the SAT rejection power. To avoid this an additional detector for γ detection is foreseen.

To estimate our sensitivity on the measurement we have performed an extensive Monte Carlo simulation which tracks the outgoing electron from the interaction point to various locations along the machine layout. The result [12] of the simulation is reported in Fig. 5 where the number of events counted by the SAT detector in the single tag mode in function of the $\gamma\gamma$ mass is shown for one year running. Assuming the chiral two loop cross section from reference 18 and considering only the statistical errors we can study the significance of our measurement. In Fig. 5 the cross section in mass bins of 25 MeV is reported and compared with the Crystall Ball data. It is clear that the DAΦNE measurement will be very accurate and extremely useful to evaluate the importance of the two loop corrections near threshold.

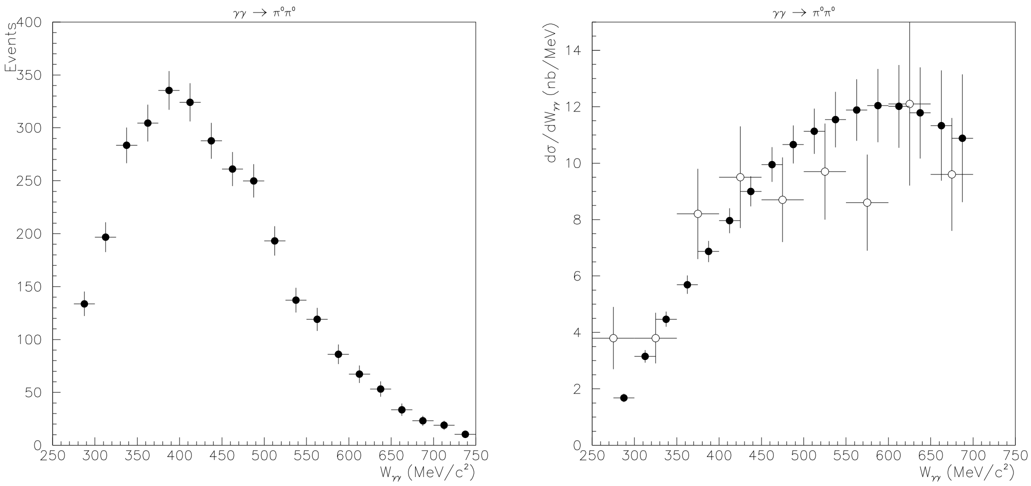

(a) (b)

Figure 5: (a) Number of $\gamma\gamma \to \pi^0\pi^0$ events, (b) cross section (black dots) compared with Crystal Ball data (open dots)

6. Conclusions

The new machine DAΦNE and the new detector KLOE will operate in the nearest future at Frascati. In addition to CP violation measurements a lot of other interesting physics can be studied.

The BR($\phi \to \gamma f_0$) can be measured down to 10^{-6} values with accuracies from a fraction of percent to 17 % at maximum. This will allow to solve the still controversial f_0, a_0 nature.

Two-photon physics can be studied with high precision due to the high statistic and the good tagging efficiency. This will allow a stringent test of chiral perturbation theory.

1. G. Vignola, *Proc. of the XXVI Int. Conf. on High Energy Physics*, ed. J. Sanford AIP (1992) 1941.
2. The KLOE Collaboration, *A general purpose detector for DAΦNE*, LNF-92/019 (1992).
3. The KLOE Collaboration, *The KLOE detector, Technical Proposal*, LNF-93/002 (1993).
4. J.Weistein, N.Isgur, Phys. Rev. Lett. **48** (1982) 659.
5. R.L.Jaffe, Phys. Rev. **D19** (1977) 267.
6. K.L.Au, D.Morgan, M.R.Pennington, Phys. Lett. **B167** (1986) 229.
7. V.N.Gribov, *Lund Preprint*, LU-TP-91-7 (1991).
8. D.Morgan, M.R.Pennington *New Data on the $K\bar{K}$ Threshold Region and the Nature of the f_0*, RAL-92-070 (1992).
9. F.Close, N.Isgur, S.Kumano, *Scalar mesons in ϕ radiative decay: Their implications for spectroscopy and for studies of CP violation at ϕ factories*, Nuclear Physics B **B389** (1993) 513.
10. J.Lee-Franzini, W.Kim, P.J.Franzini *Solving the f_0 at DAΦNE* LNF-92/055 (1992).
11. G.Alexander et al. *Two-photons physics capabilities of KLOE at DAΦNE* , LNF-93/030 (1993).
12. G.Alexander et al., *The KLOE small tagging system at DAΦNE* , KLOE-NOTE 1994-112 (1994).
13. J.Boyer et al., Phys. Rev. **D42** (1990) 1350.
14. A.Courau et al., Phys. Lett. **B96** (1980) 412.
15. Z.Ajaltouni et al., Phys. Lett. **B194** (1987) 573.
16. Ch.Berger et ale., Z. Phys. **C26** (1984) 199.
17. H.Marsiske et al., Phys. Rev **D41** (1990) 3324.
18. S.Bellucci, J.Gasser, M.Sainio, Invited talk at The Eurodafne Workshop, April 19-23, 1993.
19. M.R. Pennington, THE DAΦNE PHYSICS HANDBOOK, L.Maiani, G.Pancheri, N.Paver, Eds. (1992) 379.